INL/CON-23-75453-Revision-0

Small Hydropower Plant Response Improvement Using Energy Storage

October 2024

Yemi Ojo, W Hill Balliet, S M Shafiul Alam, Thomas Michael Rowe Mosier

Changing the World's Energy Future

INL is a U.S. Department of Energy National Laboratory operated by Battelle Energy Alliance, LLC

INL/CON-23-75453-Revision-0

Small Hydropower Plant Response Improvement Using Energy Storage

Yemi Ojo, W Hill Balliet, S M Shafiul Alam, Thomas Michael Rowe Mosier

October 2024

Idaho National Laboratory
Idaho Falls, Idaho 83415

http://www.inl.gov

Prepared for the
U.S. Department of Energy
Under DOE Idaho Operations Office
Contract DE-AC07-05ID14517

Small Hydropower Plant Response Improvement Using Energy Storage

Yemi Ojo, W Hill Balliet, S M Shafiul Alam, and Thomas M Mosier
Department of Power and Energy Systems
Idaho National Laboratory
Idaho Falls, United States
yemi.ojo@inl.gov, william.balliet@inl.gov, smshafiul.alam@inl.gov, thomas.mosier@inl.gov

***Abstract*—Small hydropower plants contribute significantly to global power generation. However, due to limited storage, these can have low ramping capacity and poor load-frequency regulation. These can prevent small hydropower plants from being used in standalone grids as backup power to critical loads and rural areas. In this paper, a control architecture for frequency control is proposed that facilitates the use of energy storage to improve the response of standalone small hydropower plants. The frequency controller generates power commands using proportional control on frequency deviation and a user-defined power setpoint, and this incorporates with a current controller that facilitates power injection. The distinctive feature of the controller design is that it takes into account frequency thresholds and storage constraints to enable power injections, and it provides the capability to perform automated and manual recharge of the energy storage. Simulations using detailed nonlinear models demonstrate the improved performance of the hydropower with energy storage using the proposed controller. Automated and manual recharge of the frequency controller, and the impact of the energy storage constraints on the performance of the hydropower plant are demonstrated.**

***Index Terms*—Small hydropower plant, energy storage, frequency control**

I. Introduction

Hydropower is a valuable source of renewable energy. Globally, small hydropower plants are expected to contribute about 11 GW by 2030 [1]. Due to seasonal changes and insufficient storage capacity, these hydropower plants can have low ramping capacity which can lead to poor load-frequency regulation. This can prevent small hydropower plants from being used for standalone microgrids to power critical infrastructures and remote areas. Therefore, improving the response of standalone small hydropower plants is a problem of practical relevance and important for increasing renewable power generation.

To improve the response of small hydropower plants, wicket gate and blade positions of hydrogovernor-turbine have been optimized to maximize power output [2]–[4]. However, due to continuous movement the hydraulic parts can suffer degradation [5], [6]. Another approach integrates hydropower plants with energy storage which incorporates controllers allowing to inject power to improve the hydropower plant response. Controllers with simple architectures have been used but these have limited functionalities, e.g., energy storage constraints are not taken into account, energy storage charges only during excess generation, and the impact of energy storage constraints on the performance of hydropower plants have not been considered [7]–[10].

In this paper, a more advanced control architecture for frequency control is proposed which allows using energy storage to improve the response of standalone small hydropower plants. The frequency controller produces power command using proportional control on frequency deviation and a user-defined power setpoint, and this incorporates with a current controller to facilitate power injection. The distinctive feature of the proposed frequency controller is that its design monitors frequency thresholds and constraints on the energy storage state-of-charge (SOC) to enable power injections. Its design provides the capability to perform automated recharge during excess generation and also gives the user the capability to perform manual recharge provided that certain operating conditions are met. These capabilities and the improved performance of the hydropower plant with energy storage using the proposed controller are demonstrated via simulations using detailed models. The impact of energy storage constraints on the performance of the hydropower plant is also demonstrated.

The remainder of this paper is organized as follows. Section II presents the physical models of the energy storage system and hydropower plant. The frequency control policy is designed in Section III. Section IV presents the simulation results and conclusions are given in Section V.

II. Modelling

In this section, the system setup of the hydropower plant with energy storage is described (Fig. 1). The hydropower plant, energy storage and load, P_L, are connected at the point of common coupling (PCC). The energy storage consists of the energy storage, a bi-directional inverter (DC-AC converter) and its current controller, and the frequency control policy. The energy storage injects[1] power into the grid at the PCC. The active power, P_{ess}, being injected is generated by the frequency control policy (Section III), which is incorporated into the inverter current controller. The hydropower plant forms the grid while the storage-side inverter tracks its frequency, ω, via a frequency measuring (FM) device.

This work is supported by the U.S. Department of Energy's Water Power Technology Office under the HydroWIRES Initiative. The project is managed by Battelle Energy Alliance, LLC under Contract No. DE-AC07-05ID14517.
The control architecture in this work is patent pending.

[1]The power injected can be of positive or negative values, where positive values implies that power flows from the energy storage to the grid, and negative values when power flows from the grid to the energy storage.

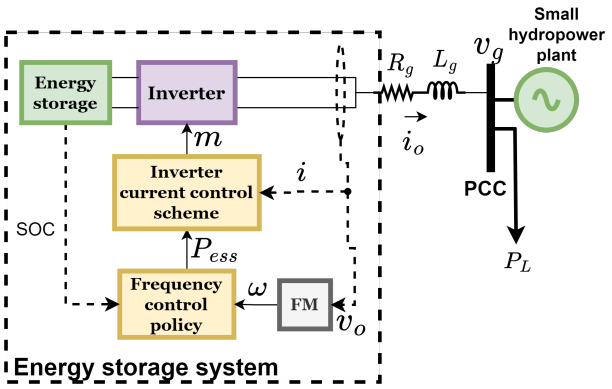

Figure 1. Standalone small hydropower plant with energy storage.

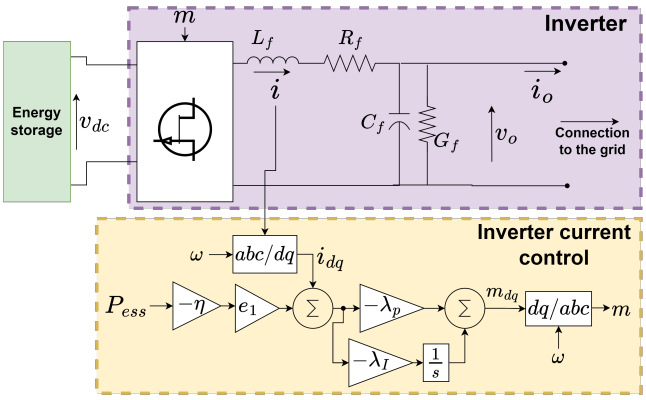

Figure 2. Inverter and its current control scheme.

A. Inverter Model

The schematic of the three-phase inverter and its current controller is shown above (Fig. 2). The DC-side of the inverter connects to the energy storage and its AC-side connects to the grid. The AC-side has an LC filter with inductance, L_f, resistance, R_f, and a shunt capacitance and conductance, C_f, G_f, respectively. The filter current, i, and voltage, v_o, are balanced three-phase sinusoidal signals. m is a balanced three-phase sinusoidal modulating signal used for the pulse-width modulation that actuates the electronic switches. To present the inverter model, it is assumed that the switching frequency is high and harmonics are attenuated. Thus, the physical abc model of the inverter is described by its average model, and its representation in the dq frame (see e.g., [11]) is given by

$$\begin{aligned} L_f \dot{i}_{dq} &= (-R_f \mathbf{I}_2 + \omega L_f J) i_{dq} + \frac{1}{2} m_{dq} v_{dc} - v_{odq} \\ C_f \dot{v}_{odq} &= (-G_f \mathbf{I}_2 + \omega C_f J) v_{odq} + i_{dq} - i_{odq} \end{aligned} \tag{1}$$

where i_{dq}, v_{odq} are respectively 2-dimensional inverter current, i, and voltage, v_o, in the dq reference frame. m_{dq} is the 2-dimensional modulating signal, m, in the dq reference frame, which is designed in Section III-B. ω denotes the frequency, $\mathbf{I}_2$ is an identity matrix of size 2, and $J = \begin{bmatrix} 0 & 1 \\ -1 & 0 \end{bmatrix}$.

B. Grid Connection

The energy storage is integrated with the hydropower plant by connecting the AC-side of the energy storage inverter to the grid. Let the lumped[2] inductance and resistance of the interconnection be L_g, R_g respectively (Fig. 1). Let the grid voltage, v_g, be a balanced three-phase sinusoidal signal, which is assumed to be tightly regulated. The interconnection in the dq reference frame is given by

$$L_g \dot{i}_{odq} = (-R_g \mathbf{I}_2 + \omega L_g J) i_{odq} + v_{odq} - \mathbf{e}_1 V_g \tag{2}$$

where $\mathbf{e}_1 V_g$ is the 2-dimensional grid voltage, v_g, in the dq reference frame; and $\mathbf{e}_1 = [1\ 0]^\top$.

C. Hydropower Plant Frequency Dynamics

To present the physical model of the hydropower plant, assume that the time constant of the hydropower plant electrical part is much faster than that of the mechanical part, and the hydropower plant voltage output is tightly regulated. The hydropower plant system can be described by its frequency dynamics[3] which are given by

$$M\dot{\omega} = -D\omega - P_L + P_g + P'_{ess} \tag{3a}$$

$$\dot{\alpha} = \omega - \omega_n \tag{3b}$$

$$P_g = -\hat{k}_P(\omega - \omega_n) - \hat{k}_I \alpha, \tag{3c}$$

where ω_n denotes the nominal frequency, P_g is the power injected by the hydropower plant to compensate for the frequency deviation, $\omega - \omega_n$. M, D are the inertia constant and damping coefficient, respectively; $\hat{k}_P$, $\hat{k}_I$ are the governor proportional and integral gains, respectively; and α is the integral state. P_L is the load demand. P'_{ess} is the active power injected by the energy storage at the PCC, which can be calculated as $P'_{ess} = \frac{3}{2}(\mathbf{e}_1 V_g)^\top i_{odq} = \frac{3}{2} V_g i_{od}$.

Remark 1: System resistances are generally small in practice. Hence, considering negligible losses, $P'_{ess} = P_{ess}$.

III. Proposed Frequency Control

In this section, a frequency control policy that allows using energy storage to improve hydropower plant response is proposed. Its integration with a current controller and associated stability result are also presented.

The frequency controller design involves producing active power in response to change in the frequency of the hydropower plant. The frequency controller uses a proportional control on frequency deviation and a user-defined power setpoint to produce active power commands, P_{ess}. The distinctive feature of the frequency controller is that its design takes into account frequency thresholds and constraints on the energy storage SOC to activate power injections. The controller design gives the capability to perform automated recharge during excess generation and also perform manual recharge provided some operating constraints are satisfied. The frequency controller is described by

$$P_{ess} = -(\mu_s \mu_p + \mu_r \overline{\mu}_p)\, k_P(\omega - \omega_n) + \mu_r \mu'_p P_t, \tag{4}$$

which is illustrated below (Fig. 3). The proportional control is given by the term with $\omega - \omega_n$, which is the deviation

[2] L_g, R_g also include those of the transformer used to connect the inverter AC-side to the PCC.

[3] Note that in the simulations (Section IV) the hydropower plant model used is detailed and includes an H6E-type horizontal bulb-style Kaplan turbine model developed in [12].

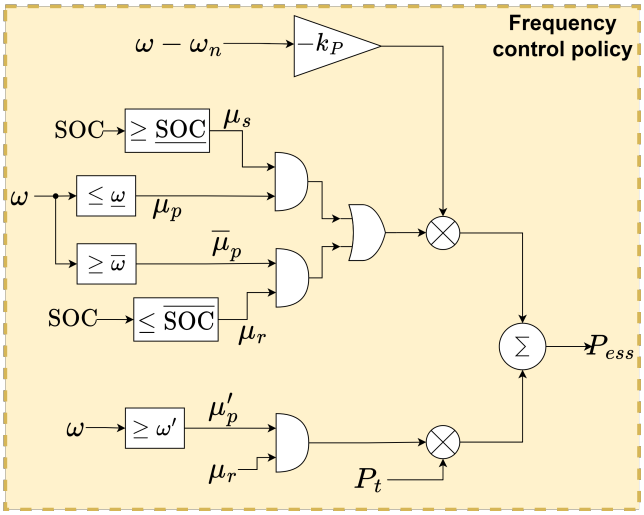

Figure 3. Proposed frequency control scheme.

of the frequency, ω, from the nominal value, ω_n. k_P is the droop gain and P_t is a user defined power command. The functions, $\mu_s, \mu_r, \mu_p, \overline{\mu}_p, \mu'_p$, allow the frequency controller (4) to take into account frequency thresholds and constraints on the energy storage SOC. These functions together with $\mu_s\mu_p + \mu_r\overline{\mu}_p$ and $\mu_r\mu'_p$ are described as follows:

- The function, μ_s, takes the value of 1 if the energy storage SOC is not below its minimum value, and of 0 if otherwise, as defined in (5).

$$\mu_s = \begin{cases} 1 & \text{for SOC} \geq \underline{\text{SOC}} \\ 0 & \text{otherwise,} \end{cases} \tag{5}$$

  where $\underline{\text{SOC}} > 0$ is the minimum SOC. The condition in (5) prevents (4) from over-discharging the energy storage.
- The function, μ_r, takes the value of 1 when the energy storage SOC satisfies SOC $\leq \overline{\text{SOC}}$, and of 0 if otherwise, as defined in (6).

$$\mu_r = \begin{cases} 1 & \text{for SOC} \leq \overline{\text{SOC}} \\ 0 & \text{otherwise} \end{cases} \tag{6}$$

  where $\overline{\text{SOC}} > 0$ is the maximum SOC. The condition in (6) prevents (4) from overcharging the energy storage.
- The function, μ_p, takes the value of 1 when the frequency, ω, is not greater than the threshold, $\underline{\omega}$, $\underline{\omega} < \omega_n$, and of 0 if otherwise, as in (7). Also, $\overline{\mu}_p$ takes the value of 1 when the frequency is not less than the threshold $\overline{\omega}$ and of 0 if otherwise, as in (8).

$$\mu_p = \begin{cases} 1 & \text{for } \omega \leq \underline{\omega},\ \underline{\omega} < \omega_n \\ 0 & \text{otherwise} \end{cases} \tag{7}$$

$$\overline{\mu}_p = \begin{cases} 1 & \text{for } \omega \geq \overline{\omega},\ \overline{\omega} > \omega_n \\ 0 & \text{otherwise} \end{cases} \tag{8}$$

  μ_p activates to allow the droop-based generation to inject power (discharge the energy storage) at a frequency, $\omega \leq \underline{\omega}$, $\underline{\omega} < \omega_n$, and $\overline{\mu}_p$ activates to allow the droop-based generation to charge the energy storage at a frequency $\omega \geq \overline{\omega}$, $\overline{\omega} > \omega_n$.
- The function, μ'_p, takes the value of 1 when the frequency, ω, is not below the threshold, ω', $\omega' < \omega_n$, and of 0 if otherwise, as in (9).

$$\mu'_p = \begin{cases} 1 & \text{for } \omega \geq \omega',\ \omega' < \omega_n \\ 0 & \text{otherwise} \end{cases} \tag{9}$$

  μ'_p activates to allow the user defined power command, $P_t < 0$, to recharge the energy storage at a frequency $\omega \geq \omega'$, $\omega' < \omega_n$.
- By the properties of $\mu_s, \mu_r, \mu_p, \overline{\mu}_p$ above, the combination, $\mu_s\mu_p + \mu_r\overline{\mu}_p$, in (4) takes the value of 1 if the conditions in (5) and (7) or (6) and (8) hold, and of 0 if otherwise. Thus, $\mu_s\mu_p + \mu_r\overline{\mu}_p$ ensures that the droop-based generation in (4) does not overly discharge the energy storage for $\omega \leq \underline{\omega}$, $\underline{\omega} < \omega_n$; or overly charge the energy storage for $\omega \geq \overline{\omega}$, $\overline{\omega} > \omega_n$.
- By the properties of μ_r, μ'_p, the combination, $\mu_r\mu'_p$, in (4) takes the value of 1 if the conditions in (6) and (9) hold, and of 0 if otherwise. Hence, a user can perform manual charging with $P_t < 0$ if the conditions in (6) and (9) are satisfied.

A. Charging and Discharging Properties

As noted above, the frequency controller (4) provides the capability to discharge and charge the energy storage to improve the response of the hydropower plant. In particular, the frequency controller (4) discharges the energy storage by generating active power commands with positive values, as in $-\mu_s\mu_p\, k_P(\omega - \omega_n) > 0$ if the conditions in (5) and (7) hold. Also, the frequency controller (4) charges the energy storage by generating active power commands with negative values, as in $-\mu_r\overline{\mu}_p k_P(\omega - \omega_n) < 0$ if the conditions in (6) and (8) are satisfied, and $\mu_r\mu'_p P_t < 0$, $P_t < 0$, if the conditions in (6) and (9) hold.

The design and capabilities provided by the frequency control policy (4) differs from existing control schemes [7]–[9]. The inclusion of the functions, $\mu_s, \mu_r, \mu_p, \overline{\mu}_p, \mu'_p$, in the control design gives (4) the capability to inject power at certain frequencies and prevent over charge (discharge) of the energy storage. The presence of P_t in (4) provides the capability to perform a manual recharge of the energy storage when $P_t < 0$ and associated conditions in μ_r, μ'_p are satisfied. This is unlike the automated recharge provided by the frequency-deviation-based generation which only occurs when there is excess generation.

B. Integration with Inverter Current Control Scheme

The proposed frequency control policy (4) can be incorporated with an inverter current controller to facilitate power transfer to and from the grid. This is achieved via the design of inverter modulating signal, m_{dq}. To this end, m_{dq} is generated by the current control scheme via a proportional and integral control on the current deviation, $i_{dq} - \mathbf{e_1}\eta P_{ess}$, given by

$$\begin{aligned} \dot{\zeta}_{dq} &= i_{dq} - \mathbf{e_1}\eta P_{ess} \\ m_{dq} &= -\lambda_P(i_{dq} - \mathbf{e_1}\eta P_{ess}) - \lambda_I\zeta_{dq}, \end{aligned} \tag{10}$$

where P_{ess} is as in (4). ηP_{ess} gives the reference current being tracked by the inverter current, i_{dq}. $\eta > 0$ is given by $1/V_g$

where $V_g > 0$ denotes the amplitude of the bus voltage v_g at the PCC. ζ_{dq} is the 2-dimensional integrator state, and λ_P, λ_I are the proportional and integral gains, respectively. The current control scheme (10) is illustrated above (Fig. 2).

C. Stability

The hydropower plant (3) is stable with the frequency controller (4). To show this, assuming that the inverter-side dynamics (1)–(2), (10) are faster than those of the hydropower plant (3). Then, stability can be shown by investigating the stability of (3) with $P_{ess} = P'_{ess}$ (Remark 1), stated as follows.

Theorem 1: Consider the hydropower plant model (3) with frequency controller (4). Assuming negligible losses with $P'_{ess} = P_{ess}$. The equilibrium point of (3)–(4) is asymptotically stable.

Proof: Let $\tilde{\omega} = \omega - \omega_n$, $\tilde{\alpha} = \alpha - \alpha^s$, where (ω_n, α^s) denotes the equilibrium point of (3)–(4). The error dynamics of (3)–(4) are $\dot{\tilde{\omega}} = -(D + \hat{k}_P + (\mu_s\mu_p + \mu_r\overline{\mu}_p)\, k_P)\tilde{\omega} - \hat{k}_I\tilde{\alpha}$; $\dot{\tilde{\alpha}} = \tilde{\omega}$. Considering the Lyapunov-like function, $\mathcal{V}(\tilde{\omega}, \tilde{\alpha}) = \frac{1}{2}M\tilde{\omega}^2 + \frac{1}{2}\hat{k}_I\tilde{\alpha}^2$, the time-derivative of $\mathcal{V}$ along the the trajectories of the error dynamics is $\dot{\mathcal{V}} = -(D + \hat{k}_P + (\mu_s\mu_p + \mu_r\overline{\mu}_p)\, k_P)\tilde{\omega}^2$. $\dot{\mathcal{V}} \leq 0$ holds since $(D + \hat{k}_P + (\mu_s\mu_p + \mu_r\overline{\mu}_p)\, k_P) > 0$ for all the values of $\mu_s, \mu_p, \mu_r, \overline{\mu}_p$ in (5)–(9). Since $\mathcal{V}$ is positive definite and radially unbounded, its level sets form compact invariant set with respect to (3)–(4). Since $(D + \hat{k}_P + (\mu_s\mu_p + \mu_r\overline{\mu}_p)\, k_P) > 0\ \forall \mu_s, \mu_p, \mu_r, \overline{\mu}_p$, $\dot{\mathcal{V}} = 0$ holds when $\tilde{\omega} = 0$. The only point of the error dynamics that corresponds to $\tilde{\omega} = 0$ is when $\tilde{\alpha} = 0$. This implies that $\omega = \omega_n, \alpha = \alpha^s$. It follows from LaSalle's theorem [13] that the equilibrium point of (3)–(4) is asymptotically stable. □

IV. Simulation Results

Simulations are performed to demonstrate the improved performance of the hydropower plant with energy storage using the proposed frequency control policy (4). Automated and manual recharging capabilities of the proposed controller (4) are investigated as well as the impact of energy storage constraints on the performance of the hydropower plant. The system setup used in the investigation is as discussed above (Fig. 1). The inverter uses the current controller (10) which incorporates the frequency control policy (4). The hydropower plant model includes an IEEE type 1 voltage regulator with exciter, a proportional-integral-based governor control as in (3b)–(3c), and an H6E-type horizontal bulb-style Kaplan turbine model as in [12]. The hydropower plant uses an 8.9 MVA 13.8 kV synchronous generator. The inverter AC-side is connected to the PCC via a 500 kVA 0.48 kV/13.8 kV transformer, where the grid and inverter are connected to the high and low voltages, respectively. A battery storage is used. System parameters including the frequency thresholds, SOC limits, and controller parameters are given above (Table I).

A. *Test I*: Energy Storage Support with Low and High SOCs

This test demonstrates the improved response of the hydropower plant with the proposed frequency controller (4) when low and high SOC energy storage is used, and this is compared to the "Base case" (when energy storage is not used). By this also the impact of energy storage SOC on the response of the hydropower plant is investigated. For that of low and high SOCs, the energy storage starts at SOCs of 20.5% and 100%, respectively. The minimum and maximum SOC limits are $\underline{\text{SOC}}$=20%, $\overline{\text{SOC}}$=100%, respectively. The hydropower plant minimum load is 1 MW. The energy storage injection is $0.42P_{ess}$ MW where P_{ess} is in per unit values. At 10 s, a load of 0.5 MW is switched ON. With (5) and (7) satisfied, the energy storage with high SOC (Fig. 4(d)) significantly improves the frequency nadir of the hydropower plant compared to that of the Base case (Fig. 4(a)). With (5) violated in that of low SOC (Fig. 4(e)), the support provided to the hydropower plant could not be sustained. This causes the second dip in the frequency response of that of low SOC (Fig. 4(a)). Thus, the hydropower plant performance could not be improved as in that of high SOC. This shows that low SOC can hamper the support energy storage provides hydropower plants, which is expected. Note that the active power injections P_{ess}, P'_{ess} are closely matched (Fig. 4(b), (c)), as indicated in Remark 1. Furthermore, the power flow betwen the two sources is balanced, where the hydropower plant generation, P_g, ramps up as the energy storage injection, P_{ess}, ramps down (Fig. 4(b), (f)). The battery is not overdischarged (Fig. 4(d), (e)) to support the hydropower plant. This validates the capability that the proposed frequency controller provides. The system is stable in the presence of disturbances, and this is achieved with desirable performance.

Table I
System Parameters

Components	Values
Inverter	Filters: L_f=0.5 mH, R_f=3 mΩ, C_f=60 mF, G_f=0 S Control parameters: λ_P=0.3, λ_I=20
Energy storage	Rating: 600-950 V, 300 Ah
SOC limits	$\underline{\text{SOC}}$=20%, $\overline{\text{SOC}}$=100%
PCC Transformer	Primary & secondary winding: 1 mΩ, 0.03 H
Frequency controller	k_P=1.5, $\underline{\omega}$=2π(59.9) rad/s, $\overline{\omega}$=2π(60.04) rad/s, ω'=2π(59.8) rad/s, ω_n=2π(60) rad/s
Hydropower plant	$\hat{k}_P$=1.5, $\hat{k}_I$=0.08, D=0.09 pu, M=2(1.3) pu

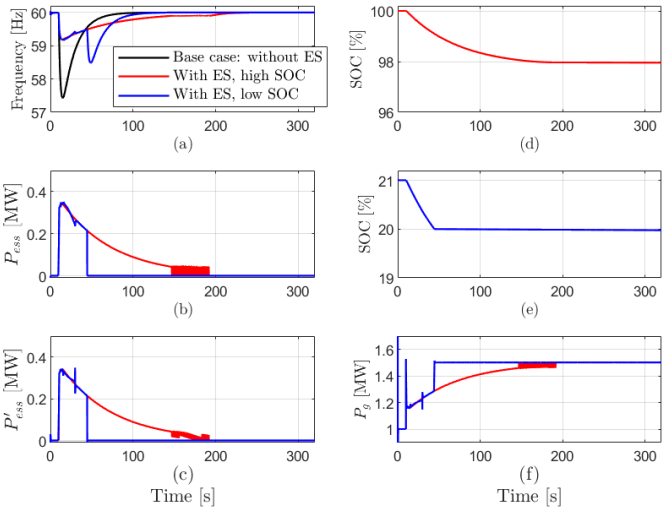

Figure 4. System response for Test I. Black line: Base case (i.e., without energy storage). Red line: with energy storage having high SOC. Blue line: with energy storage having low SOC. ES donates energy storage.

B. *Test II*: Energy Storage Support with Recharge

This test investigates the ability of the proposed frequency controller to not only perform automated recharge if (6) and (8) hold but also as desired by the user if (6) and (9) are satisfied. The test follows from Test I above. For excess generation, the 0.5 MW load is reduced by 20% at 350 s; and at 610 s, $P_t = -0.07$ pu is set in (4) to perform a manual recharge. With (6) and (8) satisfied, the energy storage recharges on the excess generation as shown by the increase in the SOC between the time, $350 \leq t \leq 475$ s (Fig. 5(d), (e)). This significantly reduces the frequency overshoot of that of low and high SOCs compared to that of the Base case (Fig. 5(a)). The negative values of P_{ess}, P'_{ess} (Fig. 5(b), (c)) show that the excess generation is absorbed by the energy storage. Note that the automated recharge stops when the frequency threshold in (8) is violated, after which the energy storage SOCs are maintained at constant values between the time, $475 \leq t \leq 600$ s (Fig. 5(d), (e)). Furthermore, with (6) and (9) satisfied, setting $P_t < 0$ at 610 s allows to perform a manual recharge of the energy storage for the time, $t > 610$ s, for that of low and high SOCs. The energy storage is fully charged to 100% (no overcharge) for that of high SOC (Fig. 6(d), while for that of low SOC the energy storage is charged to 23% (Fig. 6(e). This is validated by the negative values of P_{ess}, P'_{ess} in (Fig. 6(b), (c)), which shows that power is absorbed by the energy storage. The ability to perform the automated and manual recharge validates the capabilities that the proposed frequency controller provides, while at the same time facilitating the improved response of the hydropower plant. This is achieved with good performance and the system remains stable despite the disturbances.

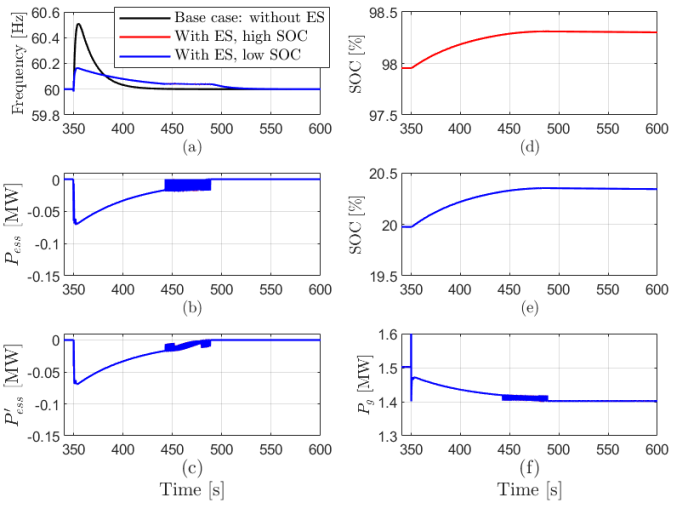

Figure 5. System response for Test II when automated recharge of the energy storage is performed. Black line: Base case (i.e., without energy storage). Red line: with energy storage having high SOC. Blue line: with energy storage having low SOC. ES donates energy storage.

V. Conclusion

Low storage limits the ramping capacity of small hydropower plants, and this can prevent their application for backup power. To remedy this issue, this paper has proposed a frequency control policy that allows using energy storage to improve the response of standalone small hydropower plants. The controller design uses frequency thresholds and SOC to decide power injection and provides the capability to perform automated and manual recharge of the energy storage. Simulations showed that the hydropower plant response is significantly improved with energy storage using the proposed controller. Future work includes the development of the proposed controller into a deployable solution, and further validations in power hardware-in-the-loop tests and on-site demonstrations with small hydropower plants.

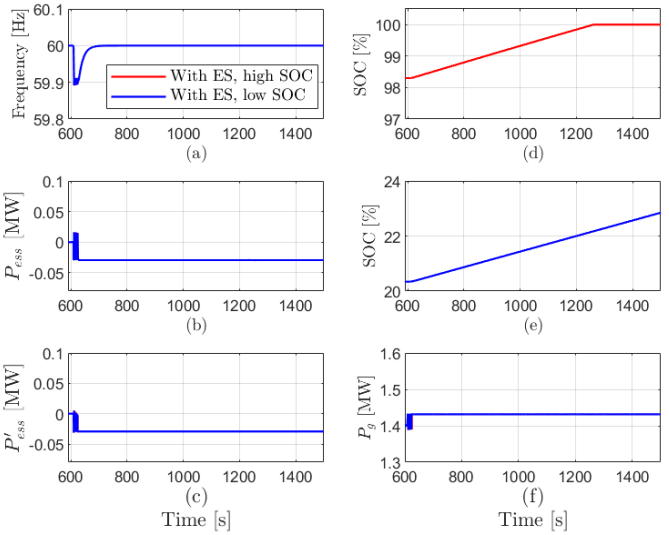

Figure 6. System response for Test II when a manual charge of the energy storage is performed. Red line: with energy storage having high SOC. Blue line: with energy storage having low SOC. ES donates energy storage.

References

[1] IEA, "Hydropower special market report—analysis and forecast to 2030." IEA Paris, France, 2021. [Online]. Available: https://www.iea.org/reports/hydropower-special-market-report

[2] M. H. Chaudhry, "Governing stability of a hydroelectric power plant," *Water Power*, vol. 22, no. 4, pp. 131–136, 1970.

[3] D. Phi *et al.*, "Analysis and application of the stability limits of a hydro-generating unit," *IEEE TPAS*, no. 7, pp. 3203–3212, 1981.

[4] D. Thorne and E. Hill, "Extensions of stability boundaries of a hydraulic turbine generating unit," *IEEE TPAS*, vol. 94, no. 4, pp. 1401–1409, 1975.

[5] W. Yang *et al.*, "Wear and tear on hydro power turbines–influence from primary frequency control," *Renewable energy*, vol. 87, pp. 88–95, 2016.

[6] K. Amiri *et al.*, "Effects of load variation on a kaplan turbine runner," *International Journal of Fluid Machinery and Systems*, vol. 9, no. 2, pp. 182–193, 2016.

[7] J. I. Sarasua *et al.*, "Hybrid frequency control strategies based on hydro-power, wind, and energy storage systems: Application to 100% renewable scenarios," *IET RPG*, vol. 16, no. 6, pp. 1107–1120, 2022.

[8] J. M. Mauricio *et al.*, "Frequency regulation contribution through variable-speed wind energy conversion systems," *IEEE TPS*, vol. 24, no. 1, pp. 173–180, 2009.

[9] A. Banerjee, S. Shafiul Alam, and T. M. Mosier, "Impact of hybrid energy storage system topologies on performance: Exploration for hydropower hybrids," in *54th HICSS*. IEEE, 2021.

[10] S. M. Shafiul Alam *et al.*, "Enhancing local grid resilience with small hydropower hybrids: Proving the concept through demonstration, simulation, and analysis with idaho falls power," 9 2022. [Online]. Available: https://www.osti.gov/biblio/1891110

[11] Y. Ojo, M. Benmiloud, and I. Lestas, "Frequency and voltage control schemes for three-phase grid-forming inverters," *IFAC-PapersOnLine*, vol. 53, no. 2, pp. 13 471–13 476, 2020.

[12] A. Banerjee *et al.*, "Modeling a bulb-style kaplan unit hydrogovernor and turbine in mathworks-simulink and rtds-rscad," in *2022 IEEE PES T&D Conference and Exposition*. IEEE, 2022, pp. 1–5.

[13] H. K. Khalil, *Nonlinear Systems*. New York, NY, USA, 3rd ed, Pearson, 2015.